Gas6 Induces Growth, β-Catenin Stabilization, and T-Cell Factor Transcriptional Activation in Contact-Inhibited C57 Mammary Cells

SANDRO GORUPPI,[1]† CRISTINA CHIARUTTINI,[1] MARIA ELISABETTA RUARO,[1]
BRIAN VARNUM,[2] AND CLAUDIO SCHNEIDER[1,3]*

*LNCIB (Laboratorio Nazionale Consorzio Interuniversitario Biotecnologie), 34012 Trieste,[1] and
Dipartimento di Scienze e Tecnologie Biomediche, Universita degli Studi di Udine,
33100 Udine,[3] Italy, and AMGEN, Inc., Thousand Oaks, California[2]*

Gas6 is a growth factor related to protein S that was identified as the ligand for the Axl receptor tyrosine kinase (RTK) family. In this study, we show that Gas6 induces a growth response in a cultured mammalian mammary cell line, C57MG. The presence of Gas6 in the medium induces growth after confluence and similarly causes cell cycle reentry of density-inhibited C57MG cells. We show that Axl RTK but not Rse is efficiently activated by Gas6 in density-inhibited C57MG cells. We have analyzed the signaling required for the Gas6 proliferative effect and found a requirement for PI3K-, S6K-, and Ras-activated pathways. We also demonstrate that Gas6 activates Akt and concomitantly inhibits GSK3 activity in a wortmannin-dependent manner. Interestingly, Gas6 induces up-regulation of cytosolic β-catenin, while membrane-associated β-catenin remains unaffected. Stabilization of β-catenin in C57MG cells is correlated with activation of a T-cell factor (TCF)-responsive transcriptional element. We thus provide evidence that Gas6 is mitogenic and induces β-catenin proto-oncogene stabilization and subsequent TCF/Lef transcriptional activation in a mammary system. These results suggest that Gas6-Axl interaction, through stabilization of β-catenin, may have a role in mammary development and/or be involved in the progression of mammary tumors.

The protein encoded by *gas6* (Gas6) is a growth factor that belongs to the vitamin K-dependent family and is closely related to the protein S and to a steroid hormone transport protein called sex hormone-binding protein (56, 57). Gas6 was reported to bind, with different affinities, to the members of the mammalian Axl receptor protein-tyrosine kinase (RTK) family (18, 34, 88). The Axl family includes Axl (named also Ark, Ufo, or Tyro7) (45, 69, 77), Rse (also named Sky, Brt, Tif, Dtk, or Tyro3) (50, 51, 86), and Mer (also named Eyk, Nyk, and Tyro12) (38, 46). Axl, Rse, and Mer are widely expressed in the adult and are present in variable amounts in neural, lymphoid, vascular, and reproductive tissues; however, their function is largely unknown. Activation of their kinase activity by Gas6 was reported to activate a mild mitogenic response in several primary and tumor-derived cell lines (35, 54, 66) and to efficiently prevent apoptosis (10, 35, 37, 67). Accordingly, simultaneous inactivation of Axl, Tyro3, and Mer in the mouse was recently related to infertility caused by the progressive death of differentiating germ cells (55). Axl was reported to transmit mitogenic and antiapoptotic signals upon Gas6 stimulation in mouse fibroblasts through a pathway involving phosphastidyl-inositol 3-kinase (PI3K) and Src (36). On this line, Mer protection of hemopoietic cells was shown to activate NF-κB and this activation was significantly suppressed by interfering with

PI3K activation (33). More recently Gas6-mediated survival was shown to activate the stress-signaling cascade and to be independent of Ras (37). The Axl-Gas6 system has been also implicated in cell-to-cell adhesion (9, 59) and chemotaxis (32). However, the role of the Axl RTK family in normal and malignant cell biology has not yet been completely elucidated. All its members are capable of inducing weak cellular transformation (38, 45, 70, 71), and Axl was reported to be overexpressed in human colon cancers (21) and in approximately 25% of primary human breast cancers (16).

β-Catenin, the mammalian homolog of *Drosophila* armadillo protein, is a protein associated with the intracellular domain of the cell junction-associated adhesion molecule cadherin (60). Through this association, β-catenin links cadherin to the actin cytoskeleton via α-catenin (11, 40). There are some indications that cell-to-cell adhesion might be negatively regulated through β-catenin phosphorylation on tyrosine residues and that this might represent an important mechanism for progression toward metastatic cancer (7, 58). Recent studies have clearly established that β-catenin represents an important signaling molecule besides its role in cadherin-mediated complexes (8, 15, 76). In fact β-catenin is involved in embryogenesis: studies carried out in *Drosophila* and *Xenopus* have demonstrated that β-catenin is a central component of the Wnt/Wingless signal transduction pathway that regulates body patterning (4, 92). In mammalian cells the transduction pathway leading from Wnt to β-catenin is not well characterized; however, several insights come from genetic analyses of the *Drosophila* homologs. Wnt signaling events are initiated by interaction with a membrane receptor of the Frizzled family, which blocks the activity of the serine/threonine kinase glyco-

gen synthase kinase 3 (GSK3), leading to stabilization of the cytoplasmic pool of β-catenin (20, 44, 74). In fact GSK3 is responsible for the phosphorylation of specific amino-terminal β-catenin residues promoting its ubiquitin-mediated degradation (1). Increase of the cytoplasmic β-catenin pool drives its interaction with the T-cell factor (TCF)/Lef family of transcription factors, resulting in altered expression of cell cycle-related genes, such as *myc* and the cyclin D1 gene (42, 75, 83).

Two mammalian GSK3 members, named α and β, have been characterized as insulin-regulated kinases involved in glycogen metabolism (22, 29, 80). GSK3 has been involved in signaling by growth factors such as insulin (23, 90), epidermal growth factor (EGF) (28, 81), and hepatocyte growth factor (scatter factor) (HGF/SF) (73). These factors provoke a rapid inactivation of GSK3 activity due to the phosphorylation of Ser21 in α and of the Ser9 residue in the β isoform. The serine/threonine kinases Akt (also called PKB) and p90 RSK have been demonstrated to be responsible for phosphorylation of these sites on GSK3 both in vitro and in vivo (23, 84). Nonetheless, only HGF/SF stimulation has been reported to induce an increase of the uncomplexed, cytosolic β-catenin pool and the consequent activation of a Lef/TCF-responsive promoter (73). In normal resting cells, GSK3 has been found in association with β-catenin, axin, and the product of the tumor suppressor gene adenomatous polyposis coli (APC) (65, 78). Several pieces of evidence suggest that β-catenin might be involved in tumorigenesis (75). Firstly, tumor-derived cell lines that lack a functional APC have higher levels of cytoplasmic β-catenin (49) and mutation, resulting in a more stable form of β-catenin, and were described in colon cancers (63) and melanomas (79). A stabilized amino-truncated β-catenin was isolated in a retroviral screening for cellular oncogenes in NIH 3T3 cells (91), and transformation of mammary cells by Wnt correlates with its regulation (82), further implicating β-catenin as a potential oncogene. In addition to these transforming abilities, overexpression of β-catenin was recently reported to confer enhanced growth in soft agar, to allow cells to cycle postconfluence, and to protect from suspension-mediated apoptosis (anoikis) in epithelial MDCK cells (72). Therefore, β-catenin may be involved in the control of cell adhesion, cell proliferation after contact inhibition, and apoptosis.

Researchers have previously characterized the mitogenic and antiapoptotic signaling activated by Gas6-Axl interaction in serum-starved NIH 3T3 cells (35, 36, 37). Gas6 was reported to act similarly as a growth factor for several different cell types under serum starvation (53, 54, 67). The purpose of this work was to identify cellular targets responding to Gas6 in the presence of high concentrations in serum in the medium. We found that C57MG mammary epithelial cells show a significant proliferative response after the addition of Gas6 to the culture medium. We have analyzed the signaling required for such a Gas6 proliferative effect and found a requirement for PI3K, S6K, and Ras-activated pathways. Interestingly, adding Gas6 to density-inhibited C57MG cells resulted in the stabilization of proto-oncogene β-catenin protein and in the activation of TCF/Lef-dependent transcription.

MATERIALS AND METHODS

Cell culture. Rat embryo fibroblasts (REF), rat smooth muscle cells (SMC), human fibroblasts (IMR90), human osteosarcoma cells (SAOS), human mammary cells (MCF7), murine fibroblasts (NIH 3T3), and mammary epithelial (C57MG) cells were routinely grown in Dulbecco's modified Eagle medium (DMEM) supplemented with 10% fetal calf serum (FCS), penicillin (100 U/ml), and streptomycin (100 μg/ml). For cell proliferation experiments, cells were seeded at 10^4 cells per cm^2 in a 6-cm-diameter petri dish. After 24 h from plating in 10% FCS, 400 ng of recombinant Gas6/ml was added to the medium for 3 days. After this time, 0.5 mg of MTT (3-[4,5-dimethyltiazol-2-yl]-2,5-diphenyltetrazoliumbromide)/ml was added to the cells to monitor the cell number and incubated for 4 h at 37°C. Labeling was stopped by adding 10% sodium dodecyl sulfate (SDS)–0.01% HCl at room temperature. Absorbance was measured at a wavelength of 595 nm. All the experiments were carried out in duplicate.

To measure growth beyond confluence, C57MG cells were similarly seeded in 6-cm-diameter petri dishes and the labeling with MTT was performed on days 0, 1, 2, and 3 in the presence or absence of 400 ng of Gas6/ml in the culture medium. The increase in cell number was evaluated after removal of the medium, a brief rinse with phosphate-buffered saline (PBS), and trypsinization. Counting was performed using a bright-light hemacytometer Neubauer chamber (Sigma). All the experiments were carried out in duplicate.

DNA synthesis assay. To measure cell growth after cell confluence, C57MG cells were plated at 10^4 per cm^2 in a petri dish containing a coverslip and were allowed to achieve density-dependent inhibition in the presence of serum for 3 days. After this time, incubation for 1 h with 50 μM BromodeoxyUridine (BrdU) (Fluka) resulted in less than 5% of nuclei being BrdU positive. The ability to induce DNA synthesis was tested by adding the indicated growth factors directly to the starvation medium together with 50 μM BrdU. After 20 h cells were fixed with 3% paraformaldehyde (Fluka) in PBS and were processed for immunofluorescence as described previously (35). For immunofluorescence, mouse monoclonal antibody anti-BrdU (Amersham, Little Chalfont, United Kingdom) was used followed by fluorescein isothiocyanate (FITC)-conjugated anti-mouse immunoglobulin G (Southern Biotechnology). Total nuclei were visualized by staining with propidium iodide (PI) (2 mM PI in PBS containing 400 μg of RNase A/ml) for 30 min at 37°C, and the coverslips were mounted using Mowiol mounting solution before analysis. The percentage of S-phase induction was calculated as the ratio between nuclei positive for FITC (BrdU) and total nuclei (PI). When wortmannin (100 nM), LY294002 (10 μM), rapamycin (20 ng/ml), SB203580 (20 μM), or PD98059 (20 μM) was used, each was added to the medium for 30, 30, 30, 60, and 60 min, respectively. Wortmannin, LY294002, sodium fluoride, and sodium orthovanadate were from Sigma. Mek inhibitor PD98059 was purchased from New England BioLabs. p38 mitogen-activated protein kinase (MAPK) inhibitor SB203580 and S6K inhibitor rapamycin were from Calbiochem Novabiochem.

Recombinant Gas6 and recombinant platelet-derived growth factor (PDGFbb) were supplied by Amgen, Inc.

Western blots. Analysis of protein expression during the density-dependent growth arrest was performed by plating several petri dishes of C57MG cells and preparing the lysates after 1, 2, 3, and 4 days. After removal of the medium, cell lysates were obtained by adding 200 μl of Laemmli sample buffer directly to the 6-cm-diameter petri dish. After SDS–10% or 15% polyacrylamide gel electrophoresis (PAGE), separation proteins were blotted to nitrocellulose membranes. Membranes were decorated separately using a rabbit affinity-purified polyclonal antibody for Axl, Gas1, and p27 (Santa Cruz Biotechnology) or a goat polyclonal antibody for Rse (Santa Cruz Biotechnology), followed by incubation with a second peroxidase-conjugated antibody (Southern Biotechnology) and detection by using enhanced chemiluminescence (ECL) (Amersham). Equal amounts of total proteins were loaded for each time as assessed by using the Bio-Rad protein assay kit and by decorating a separate Western blot with antitubulin antibodies (T. Kreis).

Analysis of Akt/PKB, MAPK, and GSK3 involvement was performed using antibodies to specific phosphorylated residues of the proteins. Confluent C57MG cells were stimulated for 15 min with 400 ng of Gas6/ml, and the total cell lysates were obtained by adding SDS-PAGE loading buffer directly to the petri dish. Loading of an equal amount of total proteins was assessed by Coomassie staining of separate gels. After SDS–15% PAGE and transfer to a polyvinyldifluoridene membrane (Millipore), for Akt a rabbit polyclonal antibody specific for the phosphorylated Thr308 (New England Biolabs, Inc.) was used, while for GSK3 a rabbit polyclonal antibody recognizing the phosphorylated Ser21 and Ser9 of GSK α and β isoforms, respectively, (QCB) was used. For MAPK we used the monoclonal antibody E10 (New England Biolabs, Inc.). All primary antibodies were diluted 1:1,000 in blocking solution (20 mM Tris [pH 7.5], 100 mM NaCl, 0.01% Tween 20, 3% bovine serum albumin [Sigma]) and were incubated overnight at 4°C. As loading control, a separate Western blot was performed using a goat polyclonal anti-Akt antibody (Santa Cruz), a rabbit polyclonal anti-MAPK antibody (Santa Cruz), or a rabbit monoclonal anti-GSK3 antibody (QCB).

Western blots were made using mouse, rabbit, or goat secondary antibodies that were peroxidase conjugated (Sigma) for 1 h at room temperature and were developed using ECL solutions (Amersham).

Immunoprecipitation. For analysis of Axl and Rse tyrosine phosphorylation, C57MG cells were made confluent as described and stimulated for 15 min with 400 ng of Gas6/ml (final concentration). After this time, cells were lysed in 150 mM NaCl, 50 mM Tris (pH 7.5) and 10 μM sodium orthovanadate. Equal amounts of total protein, as determined by using the Bio-Rad protein assay kit, were used for immunoprecipitation. The lysates were immunoprecipitated using 3 μg of two different anti-Axl and -Rse antibodies recognizing either the amino or the carboxy terminus. Immunocomplexes were separated by SDS–10% PAGE and transferred to a polyvinyldifluoridene membrane (Millipore). The membrane was incubated overnight with antiphosphotyrosine monoclonal antibody PY-20 (Transduction Laboratories). The complexes were visualized with a peroxidase-conjugated anti-mouse antibody (Sigma) and ECL solutions (Amersham).

For analysis of β-catenin association experiments, confluent C57MG cells in a 10-cm-diameter petri dish were stimulated for 30 min or not stimulated with 400 ng of Gas6/ml and were lysed in 1 ml of ice-cold lysis buffer (150 mM NaCl, 50 mM Tris [pH 7.5], 1% Triton X-100, 5 mM EDTA, 2 mM sodium orthovanadate, 1 mM phenylmethylsulfonyl fluoride, and CLAP [10 μg/ml] [aprotinin, leupeptin, antipain, and pepstatin, all from Boehringer Mannheim]). Equal amounts of cell lysates were incubated with 3 μg of affinity-purified anti-pan-cadherin (Sigma), anti-GSK3 (QCB), or anti α-catenin (Transduction Laboratories) antibodies for 4 h at 4°C and then with 15 μl of Ultralink protein A (Pierce) for a further 1 h. Immunocomplexes were washed three times in lysis buffer, resolved by SDS–10% PAGE, and blotted to a nitrocellulose membrane. Western immunoblots were examined using a monoclonal anti-β-catenin antibody (Transduction Laboratories). Complexes were visualized with peroxidase-conjugated second antibodies (Southern Biotechnology) using ECL solutions (Amersham).

For the pulse-chase analysis, replicate petri dishes of untreated control cells and C57MG cells that had been stimulated overnight with Gas6 were incubated in the absence of methionine for 20 min, pulse labeled with 100 μCi of [^{35}S]methionine/ml for 30 min, and then washed twice with PBS and incubated in medium containing excess unlabeled methionine for 1 and 2 h. Cells were extracted in lysis buffer, and equivalent protein aliquots were immunoprecipitated as described above. The immunoprecipitates were boiled for 3 min in SDS loading buffer and resolved by SDS–10% PAGE. The gel was treated with Amplify solution as recommended (Amersham), dried under vacuum, and exposed to X-ray film at −80°C.

Cell fractionation and β-catenin analysis. β-Catenin protein levels were assessed in cytosolic and membranous fractions prepared by fractionation of total cellular lysates as described previously (93). Briefly, Gas6-expressing and neomycin control NIH3T3 cells were seeded in 10-cm-diameter petri dishes. One day later, the medium was replaced with 1.5 ml of fresh DMEM containing 10% FCS. The cells were allowed to grow for 3 days; after this, the cells were lysed in 500 μl of physiological buffer (PB) (10 mM Tris [pH 7.4], 140 mM NaCl, 5 mM EDTA, 2 mM dithiothreitol, 1 mM phenylmethylsulfonyl fluoride, and 10 μg of aprotinin, leupeptin, antipain, and pepstatin/ml). The cells were homogenized in PB by 30 strokes of a Dounce homogenizer, and the lysate was centrifuged with a microcentrifuge for 15 min at 3,000 rpm (500 × g) at 4°C. Membranous and cytosolic material was obtained by ultracentrifugation at 45,000 rpm (100,000 × g) for 120 min at 4°C. The supernatant was designated the cytosolic fraction. The pellets were resuspended in PB containing 0.1% SDS (150 μl per 10-cm-diameter confluent petri dish) and were designated the membranous fraction. The protein concentration in the two fractions was measured with the Bio-Rad protein determination kit. Equal amounts of membranous or cytosolic proteins were separated by SDS–10% PAGE and were blotted to a nitrocellulose membrane. The Western blotting was carried out using either anti-β-catenin (1:5,000) or anticadherin (1:1,000) monoclonal antibodies (Sigma) in PBS–5% milk. Protein expression was visualized using peroxidase-conjugated anti-mouse secondary antibodies (Sigma) and ECL solutions (Amersham).

TCF chloramphenicol acetyltransferase (CAT) assay. The reporter plasmids pTOPCAT and pFOPCAT were generously provided by Hans Clevers (University Hospital, Utrecht, The Netherlands) (49). C57MG cells were seeded in a 6-cm-diameter petri dish, and 5 μg of plasmid DNA was introduced into cells using the calcium phosphate transfection procedure. The day after transfection, 400 ng of Gas6/ml or 100 ng of PDGFbb/ml was added to the cell medium and cells were collected and resuspended in 150 μl of reaction buffer (250 mM Tris, pH 8) after a further 24 h. Crude lysates were sonicated briefly and were clarified by centrifugation (Sigma) for 10 min at 4°C. The proteins in the supernatants were evaluated using the Bio-Rad protein assay. Equal amounts of total proteins were incubated with 3 μl of D-threo-(dichloroacetyl-1-^{14}C) chloramphenicol

(Amersham) and 0.5 μl of 40 mM acetyl coenzyme A (Sigma) for 1 h at 37°C. After this time the lipids were extracted by adding 800 μl of ethyl acetate (Sigma). The supernatants were dried and resuspended with 20 μl of ethyl acetate. Thin-layer chromatography was run on a 0.25-mm-thickness silica gel (Macherey-Nagel) in a methanol-chloroform (95%:5% [vol/vol]) saturated chamber.

Stable expressing cell lines. To obtain Gas6 stable expressing cell lines, pGDSV7gas6 and pWL-neo (Stratagene) plasmids were transfected by using the calcium phosphate procedure in NIH3T3 cells. Selection was performed by culturing for 2 weeks in the presence of 1 mg of G418 (Gibco)/ml. G418-resistant colonies were clonally expanded, and Gas6 expression was analyzed by Western blotting of total cellular lysates using specific anti-Gas6 antibodies. Immunoprecipitation of metabolically labeled Gas6 was performed essentially as described previously (56).

RESULTS

Gas6 induces cell growth after confluence of C57MG mammary cells. In order to identify Gas6 proliferation-responsive mammalian cells, several cell lines from mouse, rat, and human were screened by analyzing the effects of Gas6 in the medium. The day after seeding in a 6-cm-diameter petri dish, 400 ng of of Gas6/ml was added to the medium of asynchronous cells. They were allowed to grow for another 3 days. Control cell proliferation in 10% FCS was monitored in parallel experiments. After 3 days, the number of cells present in the petri dish was evaluated by measuring the uptake of MTT for 4 h at 37°C. The results of three independent experiments are shown in Fig. 1A. From the panel of cell lines analyzed, only C57MG mammary epithelial cells clearly responded to the presence of Gas6 in 10% FCS by undergoing a significant enhancement of their growth rate (Fig. 1A). In fact C57MG cells treated with Gas6 grew more densely as a monolayer (Fig. 1A, lower panel), while addition of Gas6 to the medium did not significantly modify the growth of SMC and NIH 3T3, REF, SA0S, U20S, IMR90, 293, C0S-7, and MCF7 cells (Fig. 1A and data not shown).

We therefore decided to characterize the biological response to Gas6 in C57MG murine mammary cells. Firstly, growth of the C57MG cells was monitored by using the same assay when they reached confluence. The experiment was carried out in triplicate, and the growth rate was evaluated on multiple days (1, 2, 3, and 4) from the seeding. The day after seeding, 400 ng of of Gas6/ml was added to the medium of one series of petri dishes. The results of this experiment, reported in Fig. 1B, show that while no significant difference is found from growth factor stimulation after 1 day, as the cells reach confluence and cease proliferating, the effect of Gas6 in the medium becomes noticeable. In fact, 3 days after the addition of Gas6, a significant difference can be observed between the treated and untreated cells. To further verify the growth-enhancing ability of Gas6 for C57MG cells, we also evaluated the increase of the cell number in a similar experiment. The cells were seeded at one-half of their usual concentration in order to avoid the effects of density-dependent inhibition and were treated with 400 ng of recombinant Gas6/ml or were left untreated the day after seeding. The total cell number was counted using a hemocytometer chamber after 1, 2, 3, and 4 days. Consistent with the results shown in Fig. 1A and B, the effects of Gas6 in the culture medium were almost undetectable when the cells were actively growing but became evident as cells reached confluence (Fig. 1C). Again, under these con-
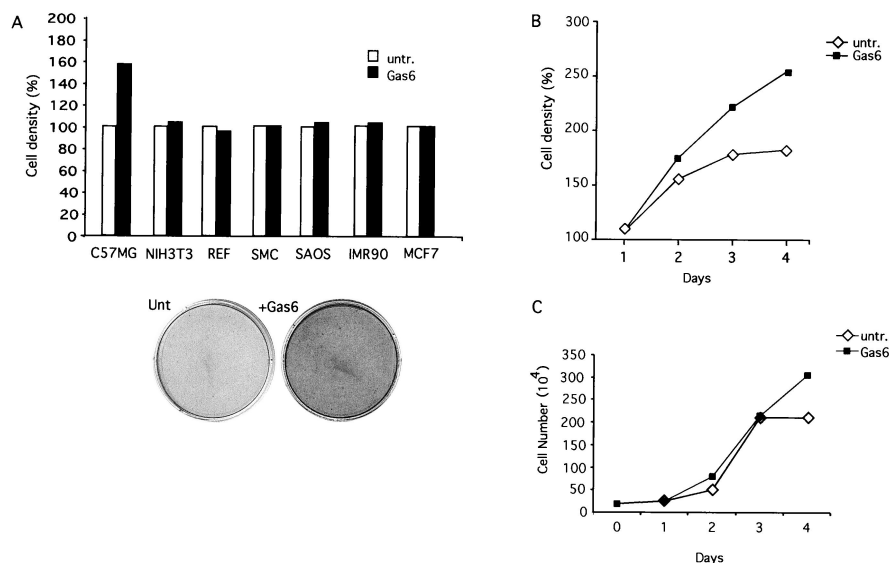
FIG. 1. Gas6 is a growth factor for C57MG cells. (A) Analysis of Gas6 growth-promoting effect on different cell lines. Cells representing REF, rat SMC, IMR90, SA0S, MCF7, NIH 3T3, and C57MG were seeded at 10^4 cells per cm^2 in 6-cm petri dishes. After 24 h from plating in 10% FCS, 400 ng of recombinant Gas6/ml was added to the medium for 3 days. After this time, MTT was added to the medium to monitor the cell number for 4 h. All the experiments were performed in duplicate at least three times. The lower panel shows the morphology of Gemsa-stained Gas6-treated C57MG cells. (B) Analysis of C57MG growth rate in the presence of Gas6. C57MG cells were similarly seeded in 6-cm-diameter petri dishes and labeled with MTT on days 1, 2, 3, and 4 after seeding in the presence or absence of 400 ng of Gas6/ml in the culture medium. (C) Analysis of Gas6-induced increase of C57MG cell number. Cells were seeded as described above at half concentration, and the increase in cell number was evaluated after 1, 2, 3, and 4 days of culture in the presence or absence of 400 ng of Gas6/ml in complete medium. After trypsinization the cells were counted using a bright-light hemacytometer Neubauer chamber (Sigma). All the experiments shown were carried out in duplicate.

ditions, addition of Gas6 circumvented the block of proliferation at confluence, with the cell number continuing to increase.

Gas6 activates the Axl receptor in confluent C57MG cells. Gas6 was first identified as the ligand for Axl RTK (88). Godowski and coworkers subsequently demonstrated that Gas6 is the ligand also for Rse/Sky, another member of the Axl RTK family (34). Western blot analysis was used to evaluate the expression of these receptors as cells became confluent. C57MG cells were seeded in 6-cm-diameter petri dishes, and at multiple times (1, 2, 3, and 4 days), total cellular lysates were obtained by directly adding SDS Laemmli loading buffer to the petri dish. After quantification, equal amounts of total proteins for each time point were analyzed by SDS-PAGE. After blotting to a nitrocellulose membrane, separate gels were probed for Axl and Rse RTK expression. As a control for density-dependent inhibition growth arrest, separate membranes were probed using antibodies to the cdk inhibitor p27 and to the growth arrest-specific Gas1 protein. Finally, Western blotting was carried out with antitubulin antibodies. Figure 2 shows the results of such analysis: both Axl RTK and Rse RTK are expressed at high levels in asynchronously growing cells and are significantly down-regulated as cells reach density-dependent growth arrest. Accordingly, p27 and Gas1 proteins are induced, confirming the block of cell proliferation by cell-to-cell contact after 3 days under these experimental conditions. The ability of Gas6 to induce Axl and Rse RTK tyrosine activation under density-dependent inhibition conditions was then assessed. Analysis of receptor phosphorylation was carried out as previously described (35). C57MG cells undergoing density-dependent growth arrest were stimulated for 10 min with 400 ng of Gas6/ml or were left untreated as a control.

After this time, the cells were lysed and the receptors were immunoprecipitated from an equal amount of total cellular proteins of stimulated and unstimulated cells, using anti-Axl or anti-Rse specific antibodies recognizing the Ct region of the receptors. Western blotting was carried out using antiphospho-tyrosine antibodies and ECL. Figure 2B shows that addition of Gas6 to the culture medium induced Axl RTK phosphorylation in C57MG cells undergoing density-dependent growth arrest. Interestingly, no significant change in Rse RTK phosphorylation was observed under the same experimental conditions. In order to confirm this finding, we performed the same experiment using a different antibody, recognizing the extracellular amino-terminal region of either Axl or Rse RTK (Fig. 2B, lower panel). Again, Axl RTK phosphorylation was significantly increased after the addition of Gas6 to cells undergoing density-dependent inhibition, but no notable changes in Rse phosphorylation were detected. Altogether, these data show that while both Axl and Rse receptors are expressed in contact-inhibited C57MG cells, only Axl is activated after the addition of Gas6, thus suggesting that Axl RTK might be responsible for the transduction of the described mitogenic signaling.

Gas6-activated signaling on density-inhibited C57MG cells. It has been previously reported that Gas6 requires PI3K-dependent signaling and S6K activity to induce cell cycle reentry of serum-starved NIH 3T3 cells (36). In this cellular context, Gas6 efficiently activates both Axl and Rse RTKs (18, 35). In order to assess whether Gas6 mitogenic activity on C57MG cells undergoing density-dependent inhibition similarly requires the previously defined pathways, we analyzed the effects of wortmannin and LY294002 as PI3K inhibitors (87). S6K
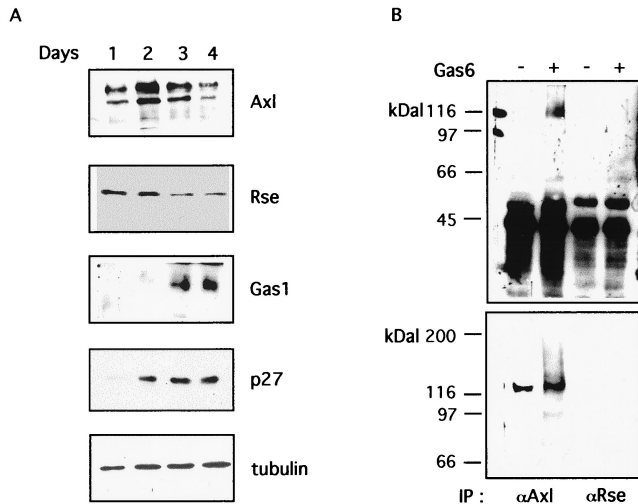
A

B

FIG. 2. Gas6 activates Axl RTK in C57MG mammary cells. (A) Analysis of Axl and Rse RTK protein expression and regulation during the assessment of density growth arrest. C57MG cells were seeded as described for Fig. 1A, and the cellular lysates were prepared after 1, 2, 3, and 4 days by adding Laemmli loading buffer directly to the petri dish. Equal amounts of total proteins, as determined using the Bio-Rad assay, were loaded on SDS-PAGE gels and were blotted to nitrocellulose membranes. Western blots were decorated separately by using rabbit affinity-purified polyclonal antibodies for Axl, Gas1, and p27; a goat polyclonal antibody for Rse; or a monoclonal antibody for tubulin. The complexes were evidenced by incubation with a secondary peroxidase-conjugated antibody and the ECL method. (B) Gas6 activates Axl RTK. Western blot analysis with antiphosphotyrosine antibodies of Axl and Rse RTKs immunoprecipitated (IP) from density-inhibited C57MG cells. Both antibodies recognizing the C-terminal region (upper panel) and the N-terminal region of Axl and Rse RTKs were used in this analysis. The results shown here are representative of several experiments. −, absence of Gas6; +, presence of Gas6.

involvement was investigated using the macrolide rapamycin, a potent inhibitor of S6K activation (19). Finally, we evaluated the requirement of Ras signaling to ERKs by using the specific Mek inhibitor PD98059 (2) and of the p38 MAPK pathway with the SB203580 inhibitor (24). In order to achieve density-dependent inhibition, C57MG cells were plated and kept in complete growth medium (DMEM–10% FCS) for 3 days. These C57MG cells were treated either with 100 nM wortmannin or with 10 μM LY294002 for 30 min and with 20 μM PD98059 or 20 μM SB203580 for 60 min before the addition of Gas6 (400 ng/ml). The S-phase entry was monitored by adding a 50 μM final concentration of BrdU at the same time as the addition of Gas6. As control, the mitogenic activity of Gas6 alone was measured in a parallel experiment. Mitogenic assays were carried out essentially as described previously (35): cells were allowed to incorporate BrdU for 20 h before immunofluorescence staining with anti-BrdU antibodies. Under these conditions, the addition of Gas6 to the culture medium induced cell cycle reentry in 30 to 40% of the cells (Fig. 3, lower panel). This mitogenic effect was, however, less than that observed with the addition of fresh 10% FCS (50% of cells positive to BrdU) that was used as a control. Blocking PI3K by adding either wortmannin or LY2940002 completely abolished Gas6-induced mitogenic activity while having no significant effects on fresh 10% FCS (not shown). Similarly, interfering with S6K activation blocked Gas6-stimulated but not FCS-

stimulated cell cycle reentry (Fig. 3 and data not shown). Moreover, treatment with the Mek inhibitor significantly inhibited Gas6-induced mitogenesis, while adding the p38 MAPK inhibitor had no significant effects on Gas6-stimulated
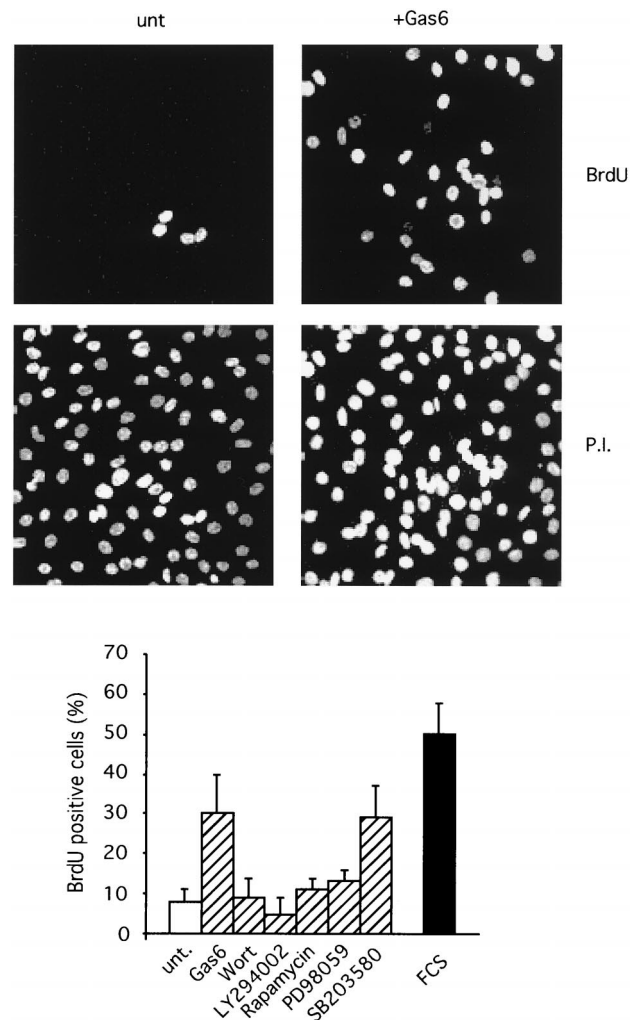

FIG. 3. Gas6 induces proliferation of density-inhibited C57MG cells. Analysis of S-phase induction in C57MG cells undergoing density-dependent inhibition. C57MG cells were plated 10^4 per cm^2 in a petri dish and were allowed to achieve density-dependent inhibition in the presence of serum (10% FCS) for 3 days. Unt, untreated. The ability to induce DNA synthesis was tested by adding 400 ng of Gas6/ml to the starvation medium together with 50 μM BrdU to monitor S-phase entry. After 20 h, cells were fixed with paraformaldehyde and processed for immunofluorescence with anti-BrdU monoclonal antibodies. Secondary antibody was anti-mouse and FITC conjugated. Total nuclei were stained with PI. When wortmannin (Wort) (100 nM), LY294002 (10 μM), rapamycin (20 ng/ml), SB203580 (20 μM), or PD98059 (20 μM) were used, each was added to the starvation medium (for 30, 30, 30, 60, and 60 min respectively) before addition of Gas6. No significant effect on 10% FCS-induced cell cycle reentry was found for these drugs (<5%). The percentage of BrdU incorporation was calculated as the ratio of nuclei positive for FITC (BrdU) and total nuclei (P.I.). The mean of four independent experiments carried out in duplicate together with the standard deviation of the mean is reported here. Immunofluorescence analysis was performed using an Axiovert 35 microscope (Zeiss), and images were obtained with a confocal laser scan microscope (Zeiss).
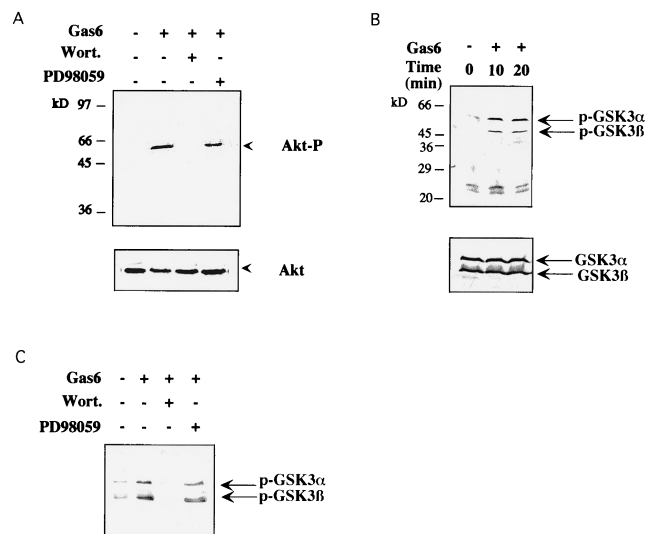
FIG. 4. Gas6 addition activates Akt and inhibits GSK3 in C57MG cells. (A) Gas6 induces the activation of Akt. Western blot analysis with antibodies specific to the threonine 308 of Akt (Akt-P) was performed on total cellular lysates from density-inhibited C57MG stimulated (+) or not (−) for 20 min with 400 ng of Gas6/ml. An identical blot was decorated with anti-Akt to monitor the total amount of the kinase in the extracts (lower panel). In separate experiments, cells were treated with 100 nM wortmannin (Wort.) or 20 μM PD98059 before addition of Gas6 to the medium. (B) Gas6 induces the inactivation of GSK3. The activation state of endogenous GSK3 α and β isoforms after Gas6 addition to C57MG cells undergoing DDI was determined by Western blotting with specific antibodies recognizing only the phosphorylated, inactive form of the kinase. Cells were stimulated for 0, 10, and 20 min before Western blot analysis. An identical Western blot was stained with anti-GSK3 antibody to monitor the total amount of the kinase in the samples (lower panel). (C) Adding wortmannin prevents Gas6-dependent GSK3 regulation. Western blot analysis of GSK3 regulation was performed as described for panel B. Total cellular lysates from density-inhibited C57MG were stimulated (+) or not (−) for 20 min with 400 ng of Gas6/ml; in separate experiments, cells were treated with 100 nM wortmannin (Wort.) or 20 μM PD98059 before addition of Gas6 to the medium.

mitogenesis. These data altogether indicate that in order for Gas6 to perform its mitogenic activity on density-inhibited C57MG cells, it requires activation of a pathway involving PI3K, S6K, and Mek.

Gas6 regulates GSK3 activity. Akt, also referred to as PKB, is a well-characterized downstream target of PI3K (17). Several growth and survival factors activate this protein kinase in a wortmannin-dependent manner by inducing its phosphorylation at the threonine 308 and serine 473 residues (26). It has been previously reported that Gas6 is able to activate Akt, this activation being insensitive to rapamycin but sensitive to wortmannin (36). In order to examine Akt involvement in Gas6-activated signaling in this system, confluent C57MG cells were stimulated for 15 min with 400 ng of Gas6/ml. Separate petri dishes were treated either with 100 nM wortmannin or with 20 μM PD98059 before the addition of Gas6 or were left untreated as controls. The cells were lysed by adding SDS loading buffer directly to the petri dishes, and Western blots were carried out using a commercial antibody specific to the activated (phosphorylated) form of Akt. Control Western analysis was performed with a specific anti-Akt polyclonal antibody in

order to visualize all Akt forms. As shown in Fig. 4A, adding Gas6 to density-inhibited C57MG cells induced a rapid activation of Akt, which was completely abolished by treatment with wortmannin. Conversely, no significant effects on Akt activation were detected when Mek inhibitor PD98059 was added to the medium. These findings, together with the described results from the mitogenic assay, suggest that Gas6 requires the activation of Akt to carry out its mitogenic activity on C57MG density-inhibited cells.

In order to obtain further insights into Gas6-stimulated mitogenesis on C57MG cells, we investigated the role of GSK3, a known downstream target of Akt. GSK3 is an enzyme, constitutively active in resting mammary cells, which is inactivated in response to stimulation by several growth factors, such as insulin, EGF, and HGP/SF (20). Akt has been shown to inactivate GSK3 through phosphorylation of the specific serine residues Ser9 and -21 in the α and β GSK3 isoforms. We therefore analyzed the ability of Axl to induce GSK3 phosphorylation after adding Gas6 to C57MG cells undergoing density-dependent inhibition. Cells were stimulated for 0, 10, and 20 min with 400 ng of Gas6/ml. After this time, cells were lysed by adding SDS loading buffer to the petri dish and equal amounts of total proteins were analyzed by Western blotting by using a polyclonal antibody specific for the phosphorylated (inactive) form of GSK3α and -β. Separate Western blots were examined to quantify GSK3 by using a monoclonal antibody raised to a sequence conserved in both α and β GSK3 isoforms. As previously reported (73), in C57MG cells α and β GSK3 isoforms are expressed as doublets of 45 and 51 kDa respectively. Figure 4B shows the results of a typical experiment indicating that a significant increase in GSK3 phosphorylation is observed after adding Gas6 to the cell medium. We can conclude that Gas6 stimulation of C57MG cells undergoing density-dependent inhibition results in down-regulation of GSK3α and -β activity.

In order to identify elements upstream of GSK3 in Gas6-activated signaling, we studied the effects of wortmannin and PD98059 in the regulation of GSK3. Confluent C57MG cells were treated with 100 nM wortmannin or 20 μM PD98059 before adding Gas6 (400 ng/ml) to monitor their respective effects on GSK3 activity. The addition of wortmannin completely blocked Gas6-induced GSK3 phosphorylation, while no significant effect on GSK3 phosphorylation was detected when cells were pretreated with PD98059 inhibitor (Fig. 4C). Our results are consistent with the reported regulation of GSK3 by other growth factors, such as insulin and PDGF, and implicate PI3K as a mediator in Gas6-dependent activation of GSK3 in C57MG cells undergoing density-dependent growth arrest.

Gas6 does not act as a growth potentiation factor for C57MG cells. Gas6 was shown to induce cell proliferation, and such growth-promoting activity was reported to be restrained in some cellular systems, as in vascular smooth muscle cells (66), in particular at higher cell density (Fig. 1 and S. Goruppi, unpublished data). This raised the hypothesis that Gas6 might not produce a full mitogenic response by itself but is merely potentiating or revealing the growth response of a factor present in the serum. We thus determined if Gas6 is able to induce cell cycle reentry under serum starvation, either at low or high cell density. To achieve serum starvation, C57MG cells were plated, and after 1 day, the culture medium was changed
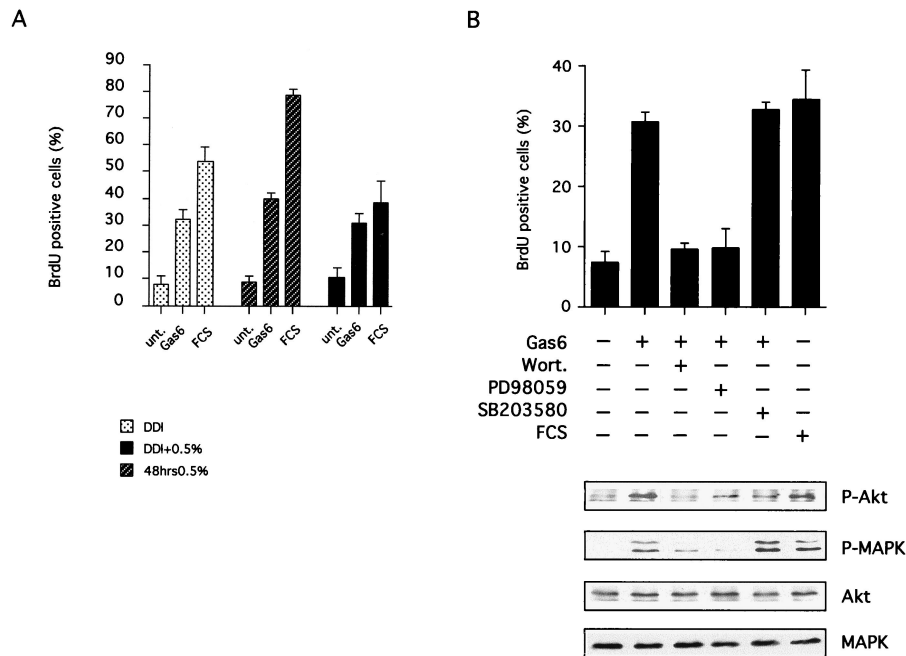
A

B

FIG. 5. Gas6 does not act as a growth-potentiating factor for C57MG cells. (A) Gas6-induced proliferation is maintained in serum-starved C57MG cells. C57MG cells were plated at 10^4 per cm^2 in 10% FCS–DMEM and were allowed to achieve DDI in the presence of serum for 3 days. Then cells were either maintained in the same medium (DDI), or the medium was changed to 0.5% FCS (DDI + 0.5%) and further incubated for 24 h. Serum-starved cells (48 h; 0.5%) were obtained by changing the medium to 0.5% FCS on the day after seeding and were incubated for 2 days. The ability to induce DNA synthesis was tested by adding to the culture medium 400 ng of Gas6/ml together with 50 μM BrdU for 20 h. An immunofluorescence assay was performed as described in Materials and Methods. Unt, untreated. (B) Analysis of Gas6-induced downstream signaling on serum-starved DDI C57MG cells. DDI + 0.5% cells were prepared and treated as described for panel A. When wortmannin (100 nM), PD98059 (20 μM), or SB203580 (20 μM) was used, each was added to the culture medium for 1 h before stimulation with Gas6 (400 ng/ml). Entry into the S phase was monitored after 20 h as described above. An analysis of Akt and MAPK activation was performed: Western blotting with antibodies specific to Thr308 of Akt (P-Akt) or raised against Thr202/Tyr204 of p44/42 MAPK (P-MAPK). C57MG cells were prepared as above, and 1 h before Gas6 stimulation, the medium was changed to serum-free DMEM. In separate experiments, cells were treated with wortmannin (100 nM), PD98059 (20 μM), or SB203580 (20 μM) before Gas6 stimulation. Parallel membranes were decorated with anti-Akt or anti-MAPK to monitor the total amount of kinase in the lysate. Cells were separately stimulated with 10% FCS and used as positive control (FCS). −, absence; +, presence.

with 0.5% FCS for 2 additional days. In separate experiments, cells were kept in complete medium after plating for 3 days to reach density-dependent inhibition before changing the medium with 0.5% FCS for an additional 24 h. Then the cells were stimulated separately with Gas6 (400 ng/ml) or FCS (10%) as a control. The S phase was monitored by adding 50 μM BrdU at the same time as Gas6. Incorporation was monitored after 20 h, as described for Fig. 3. The addition of Gas6 to serum-starved cells induced cell cycle reentry in 40% of the cells (Fig. 5). The effect was nevertheless lower than that observed in the 10% FCS-treated control cells (80% of cells positive to BrdU). In C57MG cells that were serum starved after reaching density-dependent inhibition, Gas6 similarly induced BrdU labeling of 30 to 40% of the cells (Fig. 5). The percentage of serum-starved density-dependent cells entering the S phase was analogous to the percentage obtained when density-dependent cells were stimulated with Gas6 (Fig. 3 and 5). Interestingly, the effect of Gas6 under these low-serum conditions (density-dependent inhibition [DDI] + 0.5%) was comparable to that which was observed with 10% FCS.

In order to assess whether Gas6 mitogenic activity during serum starvation requires the pathways described for C57MG cells undergoing density-dependent inhibition in the presence of serum, we analyzed the effects of wortmannin as a PI3K in-

hibitor. The requirement of Ras signaling to ERKs was evaluated by using the PD98059 inhibitor (2), while the p38 MAPK pathway was analyzed with the SB203580 inhibitor (24). C57MG cells were plated and maintained in complete medium (10% FCS) for 3 days to reach density-dependent inhibition. Then the growth medium was replaced with 0.5% FCS for 24 h before stimulation. In separate experiments, serum-starved, density-inhibited C57MG cells were treated with 100 nM worthmannin for 30 min and with 20 μM PD98059 or 20 μM SB203580 for 60 min before adding Gas6 (400 ng/ml). The S-phase entry was monitored by adding 50 μM BrdU at the same time as Gas6. As a control, the mitogenic activity of Gas6 alone was measured in a parallel experiment. Mitogenic assays were carried out after 20 h, as described for cells shown in Fig. 3. Adding Gas6 to the culture medium of serum-starved C57MG cells induced cell cycle reentry in 30% of the cells (Fig. 5B). Blocking PI3K by adding wortmannin completely abolished Gas6-induced mitogenic activity while having no significant effects on 10% FCS (not shown). Similarly, treatment with the Mek inhibitor significantly inhibited Gas6-induced mitogenesis. On the other hand, adding the p38 MAPK inhibitor had no significant effects on Gas6-stimulated mitogenesis.

We then focused on two downstream molecular targets involved in Gas6-dependent signaling: Akt, a key element in the

PI3K pathway, and MAPK, which we found to be required for density-dependent C57MG. Separate petri dishes of C57MG cells undergoing density-dependent inhibition were serum starved for 24 h and were treated with Gas6 in the presence or absence of inhibitors. When wortmannin (100 nM), PD98059 (20 μM), and SB203580 (20 μM) were used, cells were pretreated for 30, 60, and 60 min, respectively. Gas6 was added, and after 15 min, total cellular lysates were obtained by adding Laemmli SDS-PAGE loading buffer directly to the petri dishes. Equal amounts of total proteins were separated by SDS–10% PAGE and were blotted to a nitrocellulose membrane. Separate Western blotting was carried out by using a commercial antibody specific to the activated (phosphorylated) form of Akt or using a monoclonal antibody specific to activated (phosphorylated) MAPK. Control Western analysis was performed with anti-Akt or anti-MAPK polyclonal antibody in order to visualize all Akt or MAPK forms. As shown in Fig. 5B, adding Gas6 to density-inhibited, serum-starved C57MG cells induced activation of Akt, which was completely abolished by treatment with wortmannin. Conversely, no significant effects on Akt activation were detected when PD98059 or SB203580 was added to the medium. Stimulation of density-inhibited, serum-starved C57MG cells with Gas6 similarly activated MAPK, and this activation was significantly but not totally inhibited by treatment with wortmannin. As expected the Mek inhibitor PD98059 completely abolished Gas6-dependent MAPK activation. Interestingly, when cells were treated with the p38-specific inhibitor SB203580, we detected a low but reproducible increase in Gas6-induced MAPK activation.

These data, taken together, show that Gas6 mitogenic activity in C57MG cells is not dependent on the presence of serum and that during serum starvation, it activates a similar pathway involving PI3K and Mek but not p38.

Gas6 modifies β-catenin stability in C57MG cells. There is a large body of genetic and biochemical evidence showing that GSK3 functions upstream of β-catenin in the Wnt/Wingless pathway (64, 73, 89), although little is known with respect to growth factor-dependent regulation of β-catenin. In mammary cells, Wnt-activated signaling has been reported to increase protein levels of β-catenin (44). We therefore examined whether Gas6 is involved in the regulation of β-catenin protein stability. Replicate confluent monolayers of untreated control cells or C57MG cells stimulated overnight with Gas6 were pulse labeled for 30 min with [^{35}S]methionine and were then chased for 0, 1, and 2 h in the absence of the radioactive label. At each time point, total cellular lysates were prepared and protein-equivalent aliquots were immunoprecipitated with specific antibodies directed against β-catenin or Axl RTK as a control. As shown in Fig. 6A, and consistent with previous reports, β-catenin turnover was rapid in untreated density-inhibited C57MG cells. The addition of Gas6 to the culture medium led to a significant increase in the steady-state levels of β-catenin protein. Conversely, the Axl RTK half-life was shortened by adding Gas6, due to the reported increase of receptor turnover and RTK downregulation by Gas6 (88).

Previous studies have shown that a minor fraction of β-catenin is present as a free intracellular pool (73), most of it being complexed either to members of the cadherin family or to its regulating APC/GSK3/ Axin complex (75, 78, 85). To substantiate the finding that Gas6 is able to alter β-catenin protein
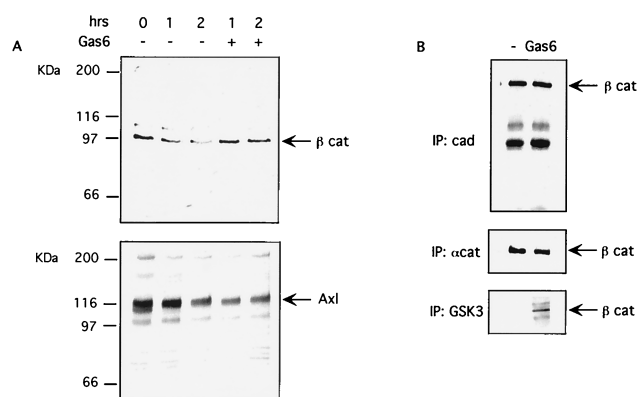

FIG. 6. Gas6 interferes with β-catenin protein stability in C57MG cells. (A) Replicate cultures of control cells (−) or C57MG cells stimulated overnight with Gas6 (+) were pulse labeled (0 h) with [^{35}S]methionine for 30 min and chased in the absence of the label for 1 and 2 h. At each time point, cellular extracts were prepared and immunoprecipitated with antibodies specific either to β-catenin (upper panel) or Axl RTK (lower panel). The immunocomplexes were analyzed by SDS-PAGE followed by fluorography. (B) Western blot analysis of β-catenin association. Confluent C57MG cells undergoing density-dependent inhibition were stimulated (Gas6) or not (−) for 30 min with 400 ng of Gas6/ml. After this time, equivalent amounts of protein extracts were immunoprecipitated with antibodies specific to either cadherins (IP:cad), α-catenin (IP αcat), or GSK3 (IP:GSK3). Immunocomplexes were resolved by SDS–10% PAGE and were blotted to nitrocellulose membranes. Western blotting was carried out with specific antibodies to β-catenin. The position of β-catenin is indicated by arrows.

stability and to dissect the target β-catenin pool, we analyzed the Gas6-induced changes in β-catenin association with GSK3, cadherin, or α-catenin; the last protein bridges β-catenin to the actin cytoskeleton. Confluent monolayers of C57MG cells were stimulated with 400 ng of of recombinant Gas6/ml for 20 min, and equivalent amounts of proteins were immunoprecipitated separately with specific monoclonal antibodies against GSK3, a monoclonal antibody against cadherin, or a monoclonal antibody against α-catenin. Immunocomplexes were separated by SDS-PAGE; after blotting, they were probed with anti-β-catenin monoclonal antibodies. Figure 6B shows that similar levels of β-catenin were associated with cadherins and α-catenin both in Gas6-stimulated and unstimulated cells. In contrast the GSK3-associated form of β-catenin could be found only after the addition of Gas6 with little or no protein being coimmunoprecipitated with GSK3 in the untreated control (Fig. 6B). No changes in β-catenin's association with cadherins or α-catenin were observed when the proteins were immunoprecipitated from cells treated for longer times (not shown). These data together show that Gas6 is able to interfere with β-catenin stability: an increase of β-catenin associated to GSK3 was found after treatment of C57MG with Gas6, consistent with the previous findings for HGF and Wnt (73).

Gas6 induces TCF4 transcriptional activation in C57MG cells. Current models suggest that cytosolic β-catenin interacts with downstream effectors as members of the TCF/Lef family which translocate to the nucleus where they activate transcription of specific target genes (39, 68). We addressed the question whether Gas6 might affect the activity of TCF/Lef transcription factors. The effects of Gas6 on TCF/Lef transcriptional activ-
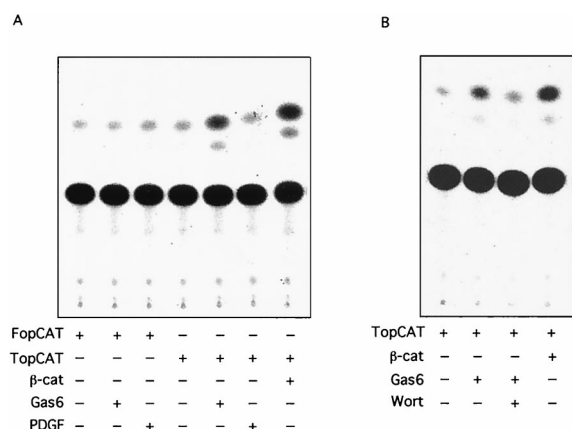
FIG. 7. Gas6 induces TCF/Lef-dependent transcription in C57MG mammary cells. (A) Gas6 induces TCF-dependent transcriptional activity. Replicate petri dishes of C57MG cells were transfected with either wt (pTOPCAT) or mutant (pFOPCAT) TCF/Lef reporter constructs (5 μg) as described in Materials and Methods. A separate petri dish was transfected simultaneously with pTOPCAT and wt β-catenin (4 μg) (β-cat) as positive control. The day after in separate experiments, either 400 ng of Gas6/ml or 100 ng of PDGFbb/ml was added to the cell medium and CAT activities were measured after 2 more days. (B) Wortmannin blocks Gas6-induced TCF-dependent transcription activation. Replicate petri dishes of C57MG cells were transfected with wild-type (pTOPCAT) TCF/Lef reporter constructs (5 μg). A separate petri dish was transfected simultaneously with pTOPCAT and wild-type β-catenin (4 μg) (β-cat) as positive control. One day later in separate experiments, either 400 ng of Gas6/ml or Gas6 and 1 μM wortmannin (Wort) were added to the cell medium and CAT activities were measured after 2 more days. The thin layer-chromatography in this figure is representative of three separate experiments.

ities on C57MG cells were analyzed by using TCF reporter-containing CAT (49). The TCF reporter construct used in these experiments, pTOPCAT, contains multiple optimal TCF binding elements placed in tandem, upstream of a minimal timidine kinase promoter driving the expression of the CAT gene. The control TCF promoter, pFOPCAT, contains critical nucleotide replacements (within the binding elements) disrupting TCF interaction.

C57MG cells were transfected with either pTOPCAT or pFOPCAT by using the calcium phosphate method. One day later, fresh medium containing either Gas6 (400 ng/ml) or PDGF (100 ng/ml) was added to the cells. Separate petri dishes were cotransfected with pTOPCAT and wild-type (wt) β-catenin expression plasmid or were left untreated as controls. Cells were harvested after 24 h, and total cell lysates were normalized for equal protein content before the CAT assays. Figure 7 shows that adding Gas6 to the medium of pTOPCAT but not to that of pFOPCAT reporter plasmid-transfected C57MG cells resulted in the efficient and reproducible activation of TCF-dependent transcription. Transactivation by Gas6 was lower than that observed when wt β-catenin was cotransfected in C57MG cells. Consistent with previous reports, a low comparable level of basal transcriptional activity was found for both reporter plasmids. Interestingly, no significant change in pTOPCAT or pFOPCAT activity was detected when the medium was complemented with PDGF, a growth factor that was previously described to share a similar pathway with Gas6. Since Gas6-dependent signaling was found to be dependent on PI3K activity, we tested the effect of wortmannin on TCF-

dependent transcription. C57MG cells were transfected with pTOPCAT reporter plasmid as shown (Fig. 7A) and were treated with 1 μM wortmannin at the moment of addition of Gas6. Separate petri dishes were cotransfected with pTOPCAT and wt β-catenin expression plasmid or were left untreated as controls. Cells were lysed after 24 h, and the CAT assays were carried out as described above. Figure 7B shows that the addition of wortmannin significantly decrease Gas6-induced TCF-dependent transcription to background levels. Therefore, adding Gas6 to C57MG cells results in activation of a wortmannin-dependent signaling pathway, leading to stabilization of β-catenin protein. Such stabilized β-catenin is most probably responsible for the observed TCF/Lef transcriptional activation by Gas6.

Gas6 induces cytosolic accumulation of β-catenin protein in NIH 3T3 fibroblasts. Previously, researchers have characterized Gas6-activated signaling in the NIH 3T3 fibroblast cell line (35, 36, 37). In order to support our evidence showing that Gas6 is able to interfere with β-catenin stabilization, we analyzed the effects of constitutive Gas6 expression on β-catenin levels in NIH 3T3 cells. To this purpose, we produced stable gas6-expressing cells by transfecting asynchronous NIH 3T3 cells with pGDSV7gas6 DNA together with a plasmid containing neomycin resistance. Clones were selected for G418 drug resistance and were screened for Gas6 expression by Western blotting using a specific anti-Gas6 antibody (not shown). Several isolated positive NIH 3T3 clones (cl) were obtained, and Fig. 8A shows the immunoprecipitation analysis of the supernatant from different metabolically labelled clones, presenting variable relative amounts of Gas6 with respect to a neomycin-resistant clone (Neo) used as the control. Equal amounts of total equivalent proteins were immunoprecipitated; the clone showing the higher level of Gas6 in the medium (cl6) was selected for further analysis and was compared to the Neo clone.

The cells were seeded, and 1 day later, the medium was changed with a minimal volume of fresh culture medium in order to allow the maximal Gas6 accumulation in the supernatant. After 3 days, the cells were lysed and β-catenin protein levels were assessed in cytosolic and membranous pools prepared by fractionation of total cellular lysates as reported by Young and coworkers (93). Figure 8B shows the results of a typical Western blot analysis with anti β-catenin antibodies of cytosolic and membranous fractions of the cl6 and Neo lysates. Western blot analyses of β-catenin protein reveal a significant increase in cytosolic protein levels in Gas6-expressing cells from those in Neo control cells. β-Catenin levels remained constant in the membranous fraction. The faster-migrating band in the membranous fraction is probably due to some degradation of β-catenin during the fractionation procedure. These data confirm the findings reported for C57MG cells on β-catenin protein stabilization and indicate moreover that Gas6 interferes with the cytosolic β-catenin pool, suggesting a potential role in β-catenin-mediated signaling for Gas6.

It has been reported that serine phosphorylation of β-catenin by GSK3 targets the protein for ubiquitin-proteosome-mediated degradation. The multiubiquitinated forms of β-catenin accumulate when proteosome inhibitors are added to the cellular medium and can be observed in Western blotting as higher-molecular-weight forms (1). Interestingly, the β-catenin ubiquitination is greatly reduced in several Wnt-expressing
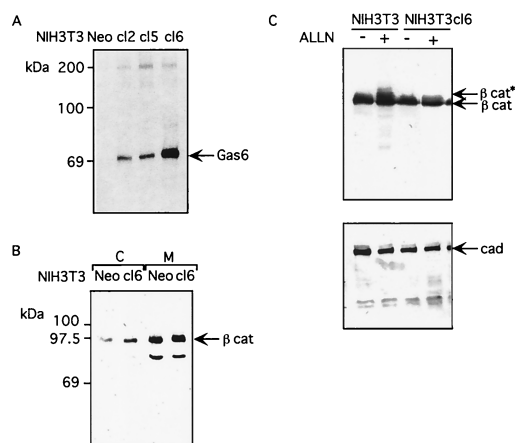
FIG. 8. Stable Gas6-expressing NIH 3T3 fibroblasts have higher cytosolic β-catenin protein levels. (A) Analysis of Gas6 expression in stable cell lines. NIH 3T3 cells were cotransfected with pGDSV7gas6 and a plasmid carrying the neomycin phosphotransferase cDNA. Relative levels of Gas6 expression were assessed by immunoprecipitating the supernatant of [³⁵S]methionine-labeled clones (cl) with specific anti-Gas6 antibodies (56). A clone transfected only with neomycin gene resistance (Neo) was used as control. The immunocomplexes were analyzed by SDS–10% PAGE followed by fluorography. (B) Gas6 induces an increase in cytosolic β-catenin protein in NIH 3T3 cells. A Western blot analysis of steady-state β-catenin protein levels in cytosolic (C) and membranous (M) protein fractions of control neomycin-expressing (Neo) and Gas6-expressing (cl6) NIH 3T3 cells was performed. Cellular extracts were prepared and fractionated, as described in Materials and Methods. Equal amounts of protein fractions were separated by SDS–10% PAGE, transferred to nitrocellulose membranes, and analyzed by Western blotting using anti-β-catenin antibody. (C) Ubiquitination of β-catenin is reduced in stable Gas6-expressing NIH 3T3 fibroblasts. Cellular lysates of control (NIH3T3) or Gas6-expressing (NIH3T3cl6) NIH 3T3 cells were treated (+) or not (−) with 25 μM ALLN for 4 h before lysis. Equal amounts of total cellular proteins were analyzed by Western blotting using anti-β-catenin antibody (upper panel) or anti-cadherin as a control (lower panel). Addition of ALLN proteosome inhibitor to cells generates higher-molecular-weight forms of β-catenin (β cat∗) but not of cadherin (cad) (1).

cell lines, confirming the link between GSK3 activity and β-catenin stability. We analyzed therefore whether constitutive Gas6 expression might lead to a decrease in β-catenin ubiquitination. To this purpose we compared the NIH 3T3 Neo clone with the Gas6-expressing cl6 clone in the presence and absence of the N-acetyl-Leu-Leu-norleucinal (ALLN) proteosome inhibitor. Cells were prepared as described for Fig. 8B, and 25 μM ALLN was added to the medium 4 h before lysis. Separate petri dishes were left untreated as the control. Lysates were obtained by adding SDS loading buffer directly to the petri dish. Equal amounts of total cellular proteins were analyzed by Western blotting with anti-β-catenin antibodies. Consistent with previous reports, adding ALLN to NIH 3T3 cells induced the accumulation of slower-migrating, higher-molecular-weight β-catenin forms. Constitutive expression of Gas6 in NIH 3T3 cells significantly reduced the presence of such slower-migrating forms. No significant changes in cadherin gel mobility were observed in either control Neo or cl6 NIH 3T3 cells (Fig. 8C, lower panel). These data are in accordance with previous findings on Wnt-expressing C57MG and NIH 3T3 cells showing that Wnt expression greatly reduced the β-catenin ubiquitination in these cells and suggest that a

decreased β-catenin turnover is similarly detected in Gas6-expressing cells.

DISCUSSION

Previous work has established that Gas6 is a potential growth and survival factor for several cellular systems. However, Gas6-dependent proliferation was mostly characterized in serum-starved fibroblasts (10, 35, 36) or after serum withdrawal (35, 67). In this study we have identified C57MG mammary epithelial cells as a Gas6-responsive cell line in high serum. We show that Gas6 induces growth of C57MG cells beyond confluence and promotes reentry into the cell cycle of cells undergoing density-dependent inhibition. We characterize part of the signaling involved in such a mitogenic response, identifying the β-catenin and TCF/Lef pathway as a target of Gas6 signaling in C57MG cells.

One proposed function of growth factors such as EGF, IGF, and PDGF is to support cell proliferation and at the same time keep control of the apoptosis machinery (6, 26, 41). Yet when untransformed cells reach confluence, new signals deriving from adjacent cells cause arrest of proliferation even in the presence of growth factors from serum (40). Among the cell lines analyzed, only C57MG continued to grow beyond confluence in the presence of Gas6. Similar to the effect of Wnt in C57MG (13, 47) and Rat-1 cells (93), Gas6 does not seem to modify the average growth rate but modifies its response to contact inhibition. A weak mitogenic response for Gas6 in mammalian cells has previously been identified in serum-starved mouse fibroblasts (35) and rat SMC (67), while the addition of Gas6 to the medium of density-inhibited cells is sufficient to induce S-phase entry only in the reported C57MG cells.

The density-dependent block of proliferation in C57MG cells was confirmed by the up-regulation of the growth-arrest-specific Gas1 protein (27) and by the expression of the p27 cdk inhibitor (43). Interestingly, the steady-state levels of both Axl and Rse receptors decrease as the cells reach density-dependent inhibition. Since C57MG cells do not express Gas6 (not shown), down-regulation of Axl and Rse might reflect the need to turn off ligand-independent receptor signaling at growth arrest. Although both receptors are expressed in C57MG, we found that only Axl was activated after the addition of Gas6 to the cells, suggesting that the mitogenic response was predominantly due to Axl receptor activation. This pointed to the possibility that the receptors of the Axl family might be responsible for different Gas6-mediated biological responses. Consistently, Gas6 does not inhibit apoptosis in fibroblasts derived from Axl knockout mice, which express physiological levels of the Rse receptor (10). However, a certain overlapping of the single receptor function might occur in vivo, since the knockout mice of either single Axl RTK family member develop normally and only the knockout mice of all the known members of the Axl RTK family have severe defects linked to the survival of reproductive and visual tissues (55). In addition to mitogenic response, Gas6 was previously reported to be involved in cell adhesion (59) and motility (32) and to prevent cell death induced by serum deprivation (10, 35), the latter probably being the most relevant in vivo (55). The ability of Gas6 to promote survival in the absence of serum for C57MG

cells was not possible to determine, since this cell line does not undergo apoptosis when challenged by serum withdrawal or DNA-damaging agents (not shown), possibly due to lack of an essential component in the cell death activation machinery.

The Axl cytoplasmic domain contains several tyrosine residues with the potential consensus for binding known molecules involved in signal transduction. Some of these tyrosines are conserved within its family members (16, 69); nevertheless, researchers have previously shown that its signaling is mainly mediated by the activity of PI3K (3, 36) through a multisubstrate docking site (14). Such a central role of PI3K in Gas6-dependent signaling was recently confirmed also for c-Mer RTK (33). By using the PI3K inhibitors wortmannin and LY294002, we showed the requirement for PI3K in Gas6 signaling in density-dependent C57MG cells. Requirement of S6K activation for Gas6-activated mitogenic response was also demonstrated: the rapamycin inhibitor abolished Gas6-induced mitogenesis in C57MG cells. Interestingly, the Gas6-dependent mitogenic response of C57MG cells undergoing density-dependent inhibition was inhibited by the PD98059 Mek inhibitor, thus indicating the requirement of the Ras-activated pathway to ERKs. These results are reminiscent of the previously characterized S-phase induction by traditional polypeptide growth factors, whereby the cell cycle reentry is driven by the Ras pathway (5, 62).

Phosphorylated lipids at the membrane in response to PI3K activation recruit the serine/threonine kinase Akt near its activating enzymes, the PDK kinases (26, 31). A previous study has demonstrated that Akt mediates growth and survival signaling as activated by several growth factors, such as PDGF and fibroblast growth factor (25, 61). A requirement of Akt kinase activity for Gas6-dependent signaling was also reported in quiescent NIH 3T3 cells (37). In order to determine new molecular targets involved in Gas6 signaling, we first analyzed the pathways of Akt activation in C57MG cells undergoing density-dependent growth arrest. This signaling was wortmannin dependent but was unaffected by Mek inhibitor treatment of the cells, indicating that the Gas6-activated pathway shares similarities with insulin- and PDGF-activated signaling (13, 23). We thus focused our attention on GSK3 kinase, a known substrate for Akt activity which becomes inactive upon phosphorylation of specific serine residues (23). In the presence of Gas6, GSK3 activity was rapidly phosphorylated in the specific serines down-regulating its activity. As observed in other cell types for insulin (23), Gas6-activated signaling to GSK3 in C57MG cells is sensitive to wortmannin, suggesting that it may occur via a PI3K-regulated step. Accordingly, inactivation of GSK3 by Gas6 is insensitive to inhibitors that prevent the activation of the classical MAPK pathway. Phosphorylation of both α and β GSK3 isoforms is similarly regulated by Gas6, which is in accord with previous studies on GSK3 inhibition by Wnt on C57MG cells (73). Our results therefore identify GSK3 as a negatively regulated target in Gas6-dependent signaling for mammary C57MG cells undergoing density-dependent inhibition. Interestingly, in a two-hybrid screen, *dishevelled* was recently reported to interact with the Tyro3 cytoplasmic domain (52). Thus, Rse/Tyro3 might also participate in other systems in GSK3 regulation, most probably in an Akt-independent manner.

Despite the fact that Gas6 was reported to elicit a prolifer-ative response, researchers (54, 66) have found that its growth-promoting potential was inhibited under certain growth conditions like high cell density. Our observation that Gas6 was able to induce proliferation only in density-arrested C57MG cells raised the possibility that it might behave as a potentiating growth factor for an unknown serum factor. In line with this hypothesis, Gas6 was reported to require a treatment of the cells with trypsin in order to induce proliferation of rat SMC (66) and a combination of heregulin and forskolin was found to be required to support maximal Schwann cell proliferation (54). When C57MG cells were deprived of serum either at low density or after reaching density-dependent inhibition, Gas6 was however able to promote cell cycle reentry as efficiently as in the presence of serum. Moreover, Gas6-activated signaling under serum starvation conditions, as defined using specific inhibitors, displayed no major differences compared to what was found when serum was present. Thus, we can conclude that the mitogenic effect observed on C57MG cells undergoing density-dependent inhibition after adding Gas6 is due to Gas6 and not to a factor present in the serum that might be depleted by certain but not all cell types. Interestingly, not even over-expression of the Axl receptor was able to unlock Gas6's proliferating potential, at least on NIH 3T3 cells (Goruppi, unpublished results). Further work will be necessary to study the molecular basis regulating the difference observed between C57MG and the other cell lines at high density; it will contribute to fully uncovering the mechanisms allowing Gas6-stimulated cells to escape density control.

A large body of evidence exists indicating that GSK3 functions upstream of β-catenin (1, 63, 64). Wnt and HGF treatment of mammary epithelial cells leads to a decrease of GSK3 activity with a parallel increase of free β-catenin pools (73). In agreement with these results, we have found that Gas6 treatment of C57MG cells increases β-catenin protein stability. As the membranous pool contains the majority of β-catenin in these cells, the total cellular β-catenin was not noticeably changed by Gas6 (not shown). In contrast to previous studies reporting an increase of β-catenin association to cadherins by Wnt (44), we found no significant changes in its junction-associated pool by Gas6. Conversely, cytosolic levels of β-catenin were found to increase after Gas6 treatment of C57MG, possibly leading to an increase in β-catenin association with the GSK3 complex. Although our anti-GSK3 antibody recognizes both α and β GSK3 isoforms, it is likely that the complex that we analyzed is associated with GSK3β, since it has been reported that GSK3β but not -α is associated with β-catenin (73). Interestingly, while previous reports have found β-catenin complexed with GSK3 also in untreated control cells (73), we were able to coimmunoprecipitate β-catenin only after Gas6 treatment. Most importantly, we have found that Gas6 is able to similarly induce stabilization of cytosolic β-catenin also in 293 cells (not shown), suggesting a more general involvement for β-catenin in Gas6-activated signaling.

Our results on the stabilization of β-catenin were further substantiated by showing that constitutive Gas6 expression in NIH 3T3 cells similarly results in an increase of its cytosolic level. Most importantly, such a cell line seems to have less β-catenin available for ubiquitination, which is in agreement with what occurs after Wnt expression in G57MG and NIH 3T3 cells (1). At present it appears that intracellular β-catenin

is mainly regulated by an active GSK3 (64). Further studies will be required to determine if in cells stably expressing Gas6, there is a constitutive down-regulation of GSK3 activity or other GSK3-independent mechanism, e.g., interaction with p85 as shown in Ras-transformed keratinocytes (30), which might be responsible for β-catenin stabilization as evidenced in our system.

The observed growth response to Gas6 in C57MG cells undergoing density-dependent inhibition is concomitant with cytosolic β-catenin induction. One proposed function of cytosolic β-catenin is interaction with TCF/Lef transcription factors that activate specific downstream genes (4, 48). We have observed that adding Gas6 to C57MG cells results in the transcriptional activation of TCF/Lef elements. Such transactivation was not confined to C57MG cells but was also detected in 293 cells (not shown). Notably, we have found that PDGF, a growth factor activating a pathway similar to that of Gas6, does not induce TCF/Lef transcriptional activation. Since the TCF/Lef promoter has been reported to be induced by some but not all growth factors sharing similar signaling pathways, it is plausible to speculate that additional elements might contribute in a positive or negative manner to their specificity for inducing β-catenin stabilization. Additional elements are required to address such "growth factor-specific" differences in β-catenin regulation. Since Gas6-induced TCF transactivation is wortmannin dependent, we can hypothesize that the pathway described here, going from Axl RTK to GSK3 through the activation of Akt, is responsible for the cytosolic β-catenin induction in this system.

Constitutive TCF/Lef transcriptional activity has been identified in several tumor-derived cell lines (49). Mutation in β-catenin or in the machinery involved in its degradation has been associated with such constitutive TCF/Lef transcriptional activity. Together, these findings suggest that deregulation of β-catenin can lead to constitutive transcriptional activation of TCF target genes, such as *myc* and the cyclin D1 gene, thus contributing to tumorigenesis. A possible interpretation for our findings is that Gas6 induces β-catenin-dependent transcriptional activity, thus contributing to the proliferative response of C57MG cells. Nevertheless, we must consider that β-catenin stabilization was also found in NIH 3T3 cells which do not respond to Gas6 at higher density. This once again suggests that while β-catenin stabilization is a more general feature of Gas6-induced response, its contribution to cell growth promotion might depend on a more defined cellular background which sets up the proliferative response to critical variations in the levels of cytosolic proto-oncogene β-catenin.

A cytosolic increase of β-catenin in response to Gas6 might have additional functions for the described growth regulation in mammary cells. In fact, overexpression of β-catenin was reported to protect cells from cell detachment-induced apoptosis (anoikis) (72), and Gas6 protects cells from apoptosis in several systems (10, 35, 67). Finally, Gas6 might be responsible for other biological functions, such as morphogenetics movements, in mammary cells in vivo. In fact, both Rse/Sky (86) and Axl (data not shown) are regulated during mouse postnatal mammary development.

Here, we identify the C57MG mammary cells as a target for Gas6-dependent signaling and provide evidence that adding Gas6 to such cells results in the stabilization of a transcriptionally active β-catenin. Its involvement in Gas6-regulated signaling could therefore indicate a potential role for Gas6 in neoplastic transformation of mammary cells, where overexpression of Axl RTK has been reported.

REFERENCES

1. **Aberle, H., A. Bauer, J. Stappert, A. Kispert, and R. Kemler.** 1997. beta-catenin is a target for the ubiquitin-proteasome pathway. EMBO J. **16:**3797–3804.
2. **Alessi, D. R., A. Cuenda, P. Cohen, D. T. Dudley, and A. R. Saltiel.** 1995. PD098059 is a specific inhibitor of the activation of mitogen-activated protein kinase kinase in vitro e in vivo. J. Biol. Chem. **270:**27489–27494.
3. **Allen, M. P., C. Zeng, K. Schneider, X. Xiong, M. K. Meintzer, P. Bellosta, C. Basilico, B. Varnum, K. A. Heidenreich, and M. E. Wierman.** 1999. Growth arrest-specific gene 6 (Gas6)/adhesion related kinase (Ark) signaling promotes gonadotropin-releasing hormone neuronal survival via extracellular signal-regulated kinase (ERK) and Akt. Mol. Endocrinol. **13:**191–201.
4. **Barker, N., P. J. Morin, and H. Clevers.** 2000. The Yin-Yang of TCF/beta-catenin signaling. Adv. Cancer Res. **77:**1–24.
5. **Barnard, D., H. Sun, L. Baker, and M. S. Marshall.** 1998. In vitro inhibition of Ras-Raf association by short peptides. Biochem. Biophys. Res. Commun. **247:**176–180.
6. **Baserga, R.** 1994. Oncogenes and the strategy of growth factors. Cell **79:**927–930.
7. **Behrens, J., L. Vakaet, R. Friis, E. Winterhager, F. Van Roy, M. M. Mareel, and W. Birchmeier.** 1993. Loss of epithelial differentiation and gain of invasiveness correlates with tyrosine phosphorylation of the E-cadherin/beta-catenin complex in cells transformed with a temperature-sensitive v-SRC gene. J. Cell Biol. **120:**757–766.
8. **Behrens, J., J. P. von Kries, M. Kuhl, L. Bruhn, D. Wedlich, R. Grosschedl, and W. Birchmeier.** 1996. Functional interaction of beta-catenin with the transcription factor LEF-1. Nature **382:**638–642.
9. **Bellosta, P., M. Costa, D. A. Lin, and C. Basilico.** 1995. The receptor tyrosine kinase ARK mediates cell aggregation by homophilic binding. Mol. Cell. Biol. **15:**614–625.
10. **Bellosta, P., Q. Zhang, S. P. Goff, and C. Basilico.** 1997. Signaling through the ARK tyrosine kinase receptor protects from apoptosis in the absence of growth stimulation. Oncogene **15:**2387–2397.
11. **Ben-Ze'ev, A., and B. Geiger.** 1998. Differential molecular interactions of β-catenin and plakoglobin in adhesion, signaling and cancer. Curr. Opin. Cell Biol. **10:**629–639.
12. **Blasband, A., B. Schryver, and J. Papkoff.** 1992. The biochemical properties and transforming potential of human Wnt-2 are similar to Wnt-1. Oncogene **7:**153–161.
13. **Brady, M. J., F. J. Bourbonais, and A. R. Saltiel.** 1998. The activation of glycogen synthase by insulin switches from kinase inhibition to phosphatase activation during adipogenesis in 3T3–L1 cells. J. Biol. Chem. **273:**14063–14066.
14. **Braunger, J., L. Schleithoff, A. S. Schulz, H. Kessler, R. Lammers, A. Ullrich, C. R. Bartram, and J. W. Janssen.** 1997. Intracellular signaling of the Ufo/Axl receptor tyrosine kinase is mediated mainly by a multi-substrate docking-site. Oncogene **14:**2619–2631.
15. **Brunner, E., O. Peter, L. Schweizer, and K. Basler.** 1997. Pangolin encodes a Lef-1 homologue that acts downstream of Armadillo to transduce the Wingless signal in Drosophila. Nature **385:**829–833.
16. **Burchert, A., E. C. Attar, P. McCloskey, Y. W. Fridell, and E. T. Liu.** 1998. Determinants for transformation induced by the Axl receptor tyrosine kinase. Oncogene **16:**3177–3187.
17. **Burgering, B. M., and P. J. Coffer.** 1995. Protein kinase B (c-Akt) in phosphatidylinositol-3-OH kinase signal transduction. Nature **376:**599–603.
18. **Chen, J. K., K. Carey, and P. J. Godowski.** 1997. Identification of Gas6 as a ligand for Mer, a neural cell adhesion molecule related receptor tyrosine kinase implicated in cellular transformation. Oncogene **14:**2033–2039.
19. **Chung, J., C. J. Kuo, G. R. Crabtree, and J. Blenis.** 1992. Rapamycin-FKBP specifically blocks growth-dependent activation of and signaling by the 70 kd S6 protein kinases. Cell **69:**1227–1236.
20. **Cook, D., M. J. Fry, K. Hughes, R. Sumathipala, J. R. Woodgett, and T. C. Dale.** 1996. Wingless inactivates glycogen synthase kinase-3 via an intracellular signalling pathway which involves a protein kinase C. EMBO J. **15:**4526–4536.

21. **Craven, R. J., L. Xu, T. M. Weiner, Y.-W. Fridell, G. A. Dent, S. Srivastava, B. Varnum, E. T. Liu, and W. C. Cance.** 1995. Receptor tyrosine kinases expressed in metastatic colon cancer. Int. J. Cancer **60:**791–797.

22. **Cross, D. A., D. R. Alessi, J. R. Vandenheede, H. E. McDowell, H. S. Hundal, and P. Cohen.** 1994. The inhibition of glycogen synthase kinase-3 by insulin or insulin-like growth factor 1 in the rat skeletal muscle cell line L6 is blocked by wortmannin, but not by rapamycin: evidence that wortmannin blocks activation of the mitogen-activated protein kinase pathway in L6 cells between Ras and Raf. Biochem. J. **303:**21–26.

23. **Cross, D. A. E., D. R. Alessi, P. Cohen, M. Andjelkovich, and B. A. Hemmings.** 1995. Inhibition of glycogen synthase kinase-3 by insulin mediated by protein kinase B. Nature **378:**785–789.

24. **Cuenda, A., J. Rouse, Y. N. Doza, R. Meier, P. Cohen, T. F. Gallagher, P. R. Young, and J. C. Lee.** 1995. SB 203580 is a specific inhibitor of a MAP kinase homologue which is stimulated by cellular stresses and interleukin-1. FEBS Lett. **364:**229–233.

25. **Datta, S. R., H. Dudek, X. Tao, S. Masters, H. Fu, Y. Gotoh, and M. E. Greenberg.** 1997. Akt phosphorylation of BAD couples survival signals to the cell-intrinsic death machinery. Cell **91:**231–241.

26. **Datta, S. R., A. Brunet, and M. E. Greenberg.** 1999. Cellular survival: a play in three Akts. Genes Dev. **13:**2905–2927.

27. **Del Sal, G., M. E. Ruaro, L. Philipson, and C. Schneider.** 1992. The growth arrest-specific gene, *gas1*, is involved in growth suppression. Cell **70:**595– 607.

28. **Eldar-Finkelman, H., R. Seger, J. R. Vandenheede, and E. G. Krebs.** 1995. Inactivation of glycogen synthase kinase-3 by epidermal growth factor is mediated by mitogen-activated protein kinase/p90 ribosomal protein S6 kinase signaling pathway in NIH/3T3 cells. J. Biol. Chem. **270:**987–990.

29. **Embi, N., D. B. Rylatt, and P. Cohen.** 1979. Glycogen synthase kinase-2 and phosphorylase kinase are the same enzyme. Eur. J. Biochem. **100:**339–347.

30. **Espada, J., M. Perez-Moreno, V. M. Braga, P. Rodriguez-Viciana, and A. Cano.** 1999. H-Ras activation promotes cytoplasmic accumulation and phosphoinositide 3-OH kinase association of beta-catenin in epidermal keratinocytes. J. Cell Biol. **146:**967–980.

31. **Franke, T. F., D. R. Kaplan, and L. W. Cantley.** 1997. PI3K: downstream AKTion blocks apoptosis. Cell **88:**435–437.

32. **Fridell, Y. W., J. Villa, Jr., E. C. Attar, and E. T. Liu.** 1998. GAS6 induces Axl-mediated chemotaxis of vascular smooth muscle cells. J. Biol. Chem. **273:**7123–7126.

33. **Georgescu, M. M., K. H. Kirsch, T. Akagi, T. Shishido, and H. Hanafusa.** 1999. The tumor-suppressor activity of PTEN is regulated by its carboxyl-terminal region. Proc. Natl. Acad. Sci. USA **96:**10182–10187.

34. **Godowski, P. J., M. R. Mark, J. Chen, M. D. Sadick, H. Raab, and R. G. Hammonds.** 1995. Reevaluation of the roles of protein S and Gas6 as ligands for the receptor tyrosine kinase Rse/Tyro3. Cell **62:**355–358.

35. **Goruppi, S., E. Ruaro, and C. Schneider.** 1996. Gas6, the ligand of Axl tyrosine kinase receptor, has mitogenic and survival activities for serum starved NIH3T3 fibroblasts. Oncogene **12:**471–480.

36. **Goruppi, S., E. Ruaro, B. Varnum, and C. Schneider.** 1997. Requirement of phosphatidylinositol 3-kinase-dependent pathway and Src for Gas6-Axl mitogenic and survival activities in NIH3T3 fibroblasts. Mol. Cell. Biol. **17:** 4442–4453.

37. **Goruppi, S., E. Ruaro, B. Varnum, and C. Schneider.** 1999. Gas6-mediated survival in NIH3T3 cells activates stress signalling cascade and is independent of Ras. Oncogene **18:**4224–4236.

38. **Graham, D. K., T. L. Dawson, D. L. Mullaney, H. R. Snodgass, and H. S. Earp.** 1994. Cloning and mRNA expression analysis of a novel human protooncogene, c-mer. Cell Growth Differ. **5:**647–657.

39. **Gumbiner, B. M.** 1995. Signal transduction of beta-catenin. Curr. Opin. Cell Biol. **7:**634–640.

40. **Gumbiner, B. M.** 1996. Cell adhesion: the molecular basis of tissue architecture and morphogenesis. Cell **84:**345–357.

41. **Guo, M., and A. H. Bruce.** 1999. Cell proliferation and apoptosis. Curr. Opin. Cell Biol. **11:**745–752.

42. **He, T. C., A. B. Sparks, C. Rago, H. Hermeking, L. Zawel, L. T. da Costa, P. J. Morin, B. Vogelstein, and K. W. Kinzler.** 1998. Identification of c-MYC as a target of the APC pathway. Science **281:**1509–1512.

43. **Hengst, L., and S. I. Reed.** 1996. Translational control of p27Kip1 accumulation during the cell cycle. Science **271:**1861–1864.

44. **Hinck, L., I. S. Nathke, J. Papkoff, and W. J. Nelson.** 1994. Dynamics of cadherin/catenin complex formation: novel protein interaction and pathways of complex assembly. J. Cell Biol. **125:**1327–1340.

45. **Janssen, J. W. G., A. S. Schultz, A. C. N. Steendoorden, M. Schmidberger, S. Strehl, P. F. Ambros, and C. R. Bartram.** 1991. A novel putative tyrosine kinase receptor with oncogenic potential. Oncogene **6:**2113–2120.

46. **Jia, R., and H. Hanafusa.** 1994. The proto-oncogene of v-eyk (v-ryk) is a novel receptor type protein tyrosine kinase with extracellular Ig/FNIII domains. J. Biol. Chem. **269:**1839–1844.

47. **Jue, S. F., R. S. Bradley, J. A. Rudnicki, H. E. Varmus, and A. M. C. Brown.** 1992. The mouse *Wnt*-1 gene can act via a paracrine mechanism in transformation of mammary epithelial cells. Mol. Cell. Biol. **12:**321–328.

48. **Kikuchi, A.** 2000. Regulation of beta-catenin signaling in the Wnt pathway. Biochem. Biophys. Res. Commun. **268:**243–248.

49. **Korinek, V., N. Barker, P. J. Morin, D. van Wichen, R. de Weger, K. W. Kinzler, B. Vogelstein, and H. Clevers.** 1997. Constitutive transcriptional activation by a beta-catenin-Tcf complex in APC−/− colon carcinoma. Science **275:**1784–1787.

50. **Lai, C., and G. Lemke.** 1991. An extended family of protein tyrosine kinase genes differentially expressed in the vertebrate nervous system. Neuron **6:** 691–704.

51. **Lai, C., M. Gore, and G. Lemke.** 1994. Structure, expression, and activity of Tyro 3, a neural adhesion-related receptor tyrosine kinase. Oncogene **9:**2567– 2678.

52. **Lan, Z., H. Wu, W. Li, S. Wu, L. Lu, M. Xu, and W. Dai.** 2000. Transforming activity of receptor tyrosine kinase tyro3 is mediated, at least in part, by the PI3 kinase-signaling pathway. Blood **95:**633–638.

53. **Lee, W.-P., Y. Liao, D. Robinson, H.-J. Kung, E. T. Liu, and M.-C. Hung.** 1999. Axl-Gas6 interaction counteracts E1A-mediated cell growth suppression and proapoptotic activity. Mol. Cell. Biol. **19:**8075–8082.

54. **Li, R., J. Chen, G. Hammonds, H. Philips, M. Armanini, P. Wood, R. Bunge, P. J. Godowski, M. X. Slikowsky, and J. P. Mather.** 1996. Identification of Gas6 as a growth factor for human Schwann cells. J. Neurosci. **16:**2012–2019.

55. **Lu, Q., M. Gore, Q. Zhang, T. Camenisch, S. Boast, F. Casagranda, C. Lai, M. K. Skinner, R. Klein, G. K. Matsushima, H. S. Earp, S. P. Goff, and G. Lemke.** 1999. Tyro-3 family receptors are essential regulators of mammalian spermatogenesis. Nature **398:**723–728.

56. **Manfioletti, G., C. Brancolini, G. Avanzi, and C. Schneider.** 1993. The protein encoded by a growth arrest-specific gene (*gas6*) is a new member of the vitamin K-dependent proteins related to protein S, a negative coregulator in the blood coagulation cascade. Mol. Cell. Biol. **13:**4976–4985.

57. **Mark, M. R., J. Chen, R. J. Hammonds, M. Sadick, and P. J. Godowsky.** 1996. Characterization of gas6, a member of the superfamily of G domain-containing proteins, as ligand for Rse and Axl. J. Biol. Chem. **271:**9785–9789.

58. **Matsuyoshi, N., M. Hamaguchi, S. Taniguchi, A. Nagafuchi, S. Tsukita, and M. Takeichi.** 1992. Cadherin-mediated cell-cell adhesion is perturbed by v-src tyrosine phosphorylation in metastatic fibroblasts. J. Cell Biol. **118:** 703–714.

59. **McCloskey, P., Y. W. Fridell, E. Attar, J. Villa, Y. Jin, B. Varnum, and E. T. Liu.** 1997. GAS6 mediates adhesion of cells expressing the receptor tyrosine kinase Axl. J. Biol. Chem. **272:**23285–23291.

60. **McCrea, P. D., and B. M. Gumbiner.** 1991. Purification of a 92-kDa cytoplasmic protein tightly associated with the cell-cell adhesion molecule E-cadherin (uvomorulin). Characterization and extractability of the protein complex from the cell cytostructure. J. Biol. Chem. **266:**4514–4520.

61. **Miho, Y., Y. Kouroku, E. Fujita, T. Mukasa, K. Urase, T. Kasahara, A. Isoai, M. Y. Momoi, and T. Momoi.** 1999. bFGF inhibits the activation of caspase-3 and apoptosis of P19 embryonal carcinoma cells during neuronal differentiation. Cell Death Differ. **6:**463–470.

62. **Molloy, C. J., D. P. Bottaro, T. P. Fleming, M. S. Marshall, J. B. Gibbs, and S. A. Aaronson.** 1989. PDGF induction of tyrosine phosphorylation of GTPase activating protein. Nature **342:**711–714.

63. **Morin, P. J., A. B. Sparks, V. Korinek, N. Barker, H. Clevers, B. Vogelstein, and K. W. Kinzler.** 1997. Activation of beta-catenin-Tcf signaling in colon cancer by mutations in beta-catenin or APC. Science **275:**1787–1790.

64. **Morin, P. J.** 1999. beta-catenin signaling and cancer. BioEssays **21:**1021–1030.

65. **Nakamura, T., F. Hamada, T. Ishidate, K. Anai, K. Kawahara, K. Toyoshima, and T. Akiyama.** 1998. Axin, an inhibitor of the Wnt signalling pathway, interacts with beta-catenin, GSK-3beta and APC and reduces the beta-catenin level. Genes Cells **3:**395–403.

66. **Nakano, T., K. Higashino, N. Kikuci, J. Kishino, K. Nomura, H. Fujita, O. Ohara, and H. Arita.** 1995. Vascular smooth muscle cell-derived, Gla-containing growth-potentiating factor for Ca(2+)-mobilizing growth factors. J. Biol. Chem. **270:**5702–5705.

67. **Nakano, T., K. Kawamoto, K. Higashino, and H. Arita.** 1996. Prevention of growth arrest-induced cell death of vascular smooth muscle cells by a product of growth arrest-specific gene, gas6. FEBS Lett. **387:**78–80.

68. **Nusse, R.** 1997. A versatile transcriptional effector of Wingless signaling. Cell **89:**321–323.

69. **O'Brian, C. A., N. E. Ward, K. R. Gravitt, and K. P. Gupta.** 1995. The tumor promoter receptor protein kinase C: a novel target for chemoprevention and therapy of human colon cancer. Prog. Clin. Biol. Res. **391:**117–120.

70. **O'Bryan, J. P., R. A. Frye, P. C. Cogswell, A. Neubauer, B. Kitch, C. Prokop, R. Espinosa III, M. M. Le Beau, H. S. Earp, and E. T. Liu.** 1991. *axl*, a transforming gene isolated from primary human myeloid leukemia cells, encodes a novel receptor tyrosine kinase. Mol. Cell. Biol. **11:**5016–5031.

71. **Ohashi, K., K. Mizuno, K. Kuma, T. Miyata, and T. Nakamura.** 1994. Cloning of the cDNA for a novel receptor tyrosine kinase, Sky, predominantly expressed in brain. Oncogene **9:**699–705.

72. **Orford, K., C. C. Orford, and S. W. Byers.** 1999. Exogenous expression of beta-catenin regulates contact inhibition, anchorage-independent growth, anoikis, and radiation-induced cell cycle arrest. J. Cell Biol. **146:**855–868.

73. **Papkoff, J., and M. Aikawa.** 1998. WNT-1 and HGF regulate GSK3 beta activity and beta-catenin signaling in mammary epithelial cells. Biochem. Biophys. Res. Commun. **247:**851–858.

74. **Peifer, M., L. M. Pai, and M. Casey.** 1994. Phosphorylation of the Drosophila

adherens junction protein Armadillo: roles for wingless signal and zeste-white 3 kinase. Dev. Biol. **166:**543–556.

75. **Peifer, M.** 1997. Beta-catenin as oncogene: the smoking gun. Science **275:** 1752–1753.

76. **Polakis, P.** 1999. The oncogenic activation of beta-catenin. Curr. Opin. Genet. Dev. **9:**15–21.

77. **Rescigno, J., A. Mansukhani, and C. Basilico.** 1991. A putative receptor tyrosine kinase with unique structural topology. Oncogene **6:**1909–1913.

78. **Rubinfeld, B., B. Souza, I. Albert, O. Muller, S. H. Chamberlain, F. R. Masiarz, S. Munemitsu, and P. Polakis.** 1993. Association of the APC gene product with beta-catenin. Science **262:**1731–1734.

79. **Rubinfeld, B., P. Robbins, M. El-Gamil, I. Albert, E. Porfiri, and P. Polakis.** 1997. Stabilization of beta-catenin by genetic defects in melanoma cell lines. Science **275:**1790–1792.

80. **Rylatt, D. B., A. Aitken, T. Bilham, G. D. Condon, N. Embi, and P. Cohen.** 1980. Glycogen synthase from rabbit skeletal muscle. Amino acid sequence at the sites phosphorylated by glycogen synthase kinase-3, and extension of the N-terminal sequence containing the site phosphorylated by phosphorylase kinase. Eur. J. Biochem. **107:**529–537.

81. **Saito, Y., J. R. Vandenheede, and P. Cohen.** 1994. The mechanism by which epidermal growth factor inhibits glycogen synthase kinase 3 in A431 cells. Biochem. J. **303:**27–31.

82. **Shimizu, H., M. A. Julius, M. Giarre, Z. Zheng, A. M. Brown, and J. Kitajewski.** 1997. Transformation by Wnt family proteins correlates with regulation of beta-catenin. Cell Growth Differ. **8:**1349–1358.

83. **Shtutman, M., J. Zhurinsky, I. Simcha, C. Albanese, M. D'Amico, R. Pestell, and A. Ben-Ze'ev.** 1999. The cyclin D1 gene is a target of the beta-catenin/LEF-1 pathway. Proc. Natl. Acad. Sci. USA **96:**5522–5527.

84. **Stambolic, V., and J. R. Woodgett.** 1994. Mitogen inactivation of glycogen synthase kinase-3 beta in intact cells via serine 9 phosphorylation. Biochem. J. **303:**701–704.

85. **Su, L. K., B. Vogelstein, and K. W. Kinzler.** 1993. Association of the APC tumor suppressor protein with catenins. Science **262:**1734–1737.

86. **Taylor, I. C., S. Roy, P. Yaswen, M. R. Stampfer, and H. E. Varmus.** 1995. Mouse mammary tumors express elevated levels of RNA encoding the murine homology of SKY, a putative receptor tyrosine kinase. J. Biol. Chem. **270:**6872–6880.

87. **Ui, M., T. Okada, K. Hazeki, and O. Hazeki.** 1995. Wortmannin as a unique probe for an intracellular signalling protein, phosphoinositide 3-kinase. Trends Biochem. Sci. **20:**303–307.

88. **Varnum, B. C., C. Young, G. Elliott, A. Garcia, T. D. Bartley, Y. W. Fridell, R. W. Hunt, G. Trail, C. Clogson, R. J. Toso, D. Yanagihara, L. Bennett, M. Sylber, L. A. Merewether, A. Tseng, E. Escobar, E. T. Liu, and H. K. Yamane.** 1995. Axl receptor tyrosine kinase stimulated by the vitamin K-dependent protein encoded by the growth-arrest-specific gene *gas6.* Nature **373:**623–626.

89. **Waltzer, L., and M. Bienz.** 1999. The control of beta-catenin and TCF during embryonic development and cancer. Cancer Metastasis Rev. **18:**231–246.

90. **Welsh, G. I., and C. G. Proud.** 1993. Glycogen synthase kinase-3 is rapidly inactivated in response to insulin and phosphorylates eukaryotic initiation factor eIF-2B. Biochem J. **294:**625–629.

91. **Whitehead, I., H. Kirk, and R. Kay.** 1995. Expression cloning of oncogenes by retroviral transfer of cDNA libraries. Mol. Cell. Biol. **15:**704–710.

92. **Willert, K., and R. Nusse.** 1998. β-catenin: a key mediator of wnt signaling. Curr. Opin. Genet. Dev. **8:**95–102.

93. **Young, C. S., M. Kitamura, S. Hardy, and J. Kitajewski.** 1998. Wnt-1 induces growth, cytosolic β-catenin, and Tcf/Lef transcriptional activation in Rat-1 fibroblasts. Mol. Cell. Biol. **18:**2474–2485.